Joint Special Interest Group meeting between euspen and ASPE
Advancing Precision in Additive Manufacturing
TU Berlin, Germany, October 2025
www.euspen.eu

Local evaluation of metal laser powder bed fusion layer-related characteristics using a metrological XCT-based methodology

F. Zanini[1], N. Bonato[1], D. Zanin[1], S. Carmignato[1]

[1]*Department of Management and Engineering, University of Padova, Vicenza, Italy*

filippo.zanini@unipd.it

Abstract
A metrological approach is proposed for local evaluation of effective layer thickness, powder bed density, and actual volumetric energy density in metal laser powder bed fusion. A custom-built plate with removable inserts enables robust alignment and accurate single-layer analysis through high-resolution metrological X-ray computed tomography (XCT). Effective layer thickness and powder bed density are determined through specifically developed procedures, allowing calculation of actual energy input. Results reveal significant deviations from nominal values and reduced energy efficiency. The method also quantifies the influence of other process-related phenomena, such as spatter formation and denudation on layer formation, offering deeper insights into process stability and efficiency.

Laser powder bed fusion; Effective layer thickness; Powder bed density; Volumetric energy density; X-ray computed tomography

1. Introduction

Improving the precision of metal laser-based powder bed fusion (PBF-LB) remains a major challenge due to its multivariable nature and the difficulty of controlling the physical phenomena involved in the laser–powder interaction [1]. Process optimization commonly relies on the volumetric energy density (VED), defined as per Eq. (1) [2].

$$VED = P/(v \cdot d \cdot NLT)\,, \quad (1)$$

where *P* is laser power, *v* scanning speed, *d* hatch distance, and *NLT* nominal layer thickness.

Studies show that the effective layer thickness (ELT) — the actual powder height involved in consolidation — can significantly exceed NLT [3]. One cause of this discrepancy is the powder bed density (PBD), quantifying the powder's mass-to-volume ratio that influences ELT and the actual energy input per unit of volume [3]. However, the ELT–NLT discrepancy is often larger than what is expected from the actual PBD, as it can be exacerbated by process-related phenomena such as denudation [4] and spattering [5], which lower the actual VED and energy efficiency. Despite its relevance, ELT has so far been measured using methods with non-robust references and not focused on local variations [3,6], which might be related to process stability and energy efficiency. PBD measurement techniques are instead typically based on multiple layers, and not on the single-layer [7].

This work investigates an experimental method enabling local, layer-specific, and simultaneous measurement of ELT, PBD, and actual VED. High-resolution metrological X-ray computed tomography (XCT) is combined with a custom-built plate featuring removable inserts with reference geometries, allowing accurate alignment and measurements [8]. The approach reveals local ELT variability, enabling spatially resolved VED assessment and deeper insight into process stability and energy conversion efficiency [9]. Reliable PBD data also allow quantifying the role of additional process-related factors, supporting more accurate evaluation and optimization of the PBF-LB process.

2. Materials and methods

The experimental approach utilized a newly designed AM building plate incorporating removable inserts featuring robust reference geometries, as shown in Fig. 1-a [8]. Inserts with 6 mm diameter protrusions enabled high-resolution XCT scanning with a 3 µm voxel size. H13 tool steel cylindrical samples with a diameter of 4 mm and height of 1.98 mm were fabricated on plate inserts using a Sisma MYSINT100 laser PBF-LB machine with the following process parameters: laser power of 120 W, scan speed of 600 mm/s, hatch distance of 0.09 mm, and NLT of 0.02 mm, corresponding to a nominal VED of 111 J/mm^3. After the fabrication, a final powder layer was deposited after lowering the platform by NLT and bonded by using cyanoacrylate adhesive.

Metrological XCT scans including sample, glued powder, and insert were performed using a Nikon Metrology MCT225 system. Data processing, including local adaptive surface determination, morphological filtering, particle analysis, alignment operations using the reference geometries on the inserts, and measurements of interest, was carried out in VGSTUDIO MAX software. Specifically, the powder bed surface topography was measured at first, as seen in Fig. 1-b. Then, the glued powder was removed by dissolution in acetone, and a new XCT scan was conducted to extract the surface topography of the last consolidated layer (Fig. 1-c). The two XCT reconstructions, with and without glued powder, were aligned to precisely isolate the powder volume and compute PBD (Fig. 1-d). The threshold value for powder particle segmentation was optimized by using a reference powder sample. The local ELT values were calculated as the distance between each point of the powder surface topography and the last layer surface, along the orthogonal direction with respect to the base plane of the insert (Fig. 1-d and 1-e).

By combining the measured mean ELT and PBD, the computed consolidated layer thickness (*CLTc*; i.e., the thickness of the consolidated material that should theoretically result from the

measured mean ELT reduced by the measured PBD) was determined as per Eq. (2), and compared to the target consolidated layer thickness (*CLTt* ≈ 0.02 mm).

$$CLT_c = \overline{ELT} \cdot PBD \quad (2)$$

The equivalent powder bed density (PBD_e), i.e., the value of PBD in the case it was the sole factor influencing the discrepancy between *CLTc* and *CLTt*, was calculated using Eq. 3.

$$PBD_e = CLT_t / \overline{ELT} \, . \quad (3)$$

By considering the impact of PBD on the discrepancy between *CLTc* and *CLTt*, it is possible to discern and quantify the complementary percentage effect of other process-related influences. Such percentage effect (ξp) can be computed as proposed in Eq. (4).

$$\xi_p = (\overline{ELT} \cdot PBD - CLT_t)/(\overline{ELT} - CLT_t) \quad (4)$$

Finally, the local actual VED was then calculated by substituting the local ELT values into the VED equation (Eq. 1).

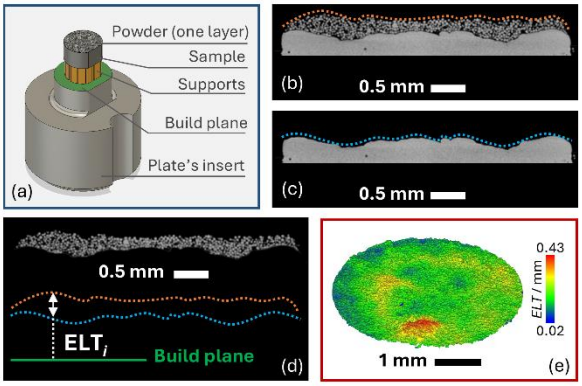

Figure 1. Representation of a plate's insert, build plane, sample, supports, and one powder layer (a). CT cross-sections showing the sample with powder glued onto the top surface (b), the sample after removing the glued powder (c), the isolated powder for PBD computation, and representation of local ELT values (ELT_i) computation (d). Example of map of ELT local values (e).

3. Results

For the investigated parameter setting as reported in Sec. 2, the mean ELT was found to be 0.170 mm, which is 8.8 times the nominal layer thickness of 0.02 mm. The distribution of local ELT values exhibited a standard deviation of 0.084 mm, indicating significant variability across the powder bed (see Fig. 2-a). This variability in ELT is linked to process stability and the ability to maintain consistent and predictable conditions at a local level for uniform melting and solidification.

The measured PBD was 65%. By combining the measured ELT and PBD, the computed consolidated layer thickness (*CLTc*) was determined to be 0.111 mm using Eq. 2.

This value deviates significantly from the target consolidated layer thickness (*CLTt*) of approximately 0.02 mm, which is expected to be similar to the NLT at steady-state conditions. The equivalent powder bed density (PBD_e) was calculated to be 12% using Eq. 3.

The PBD_e of 12% is significantly smaller than the measured PBD of 65%, indicating that other process-related factors, such as material shrinkage, spatter formation, denudation, and metal vaporization, also contribute substantially to the observed discrepancy between *CLTc* and *CLTt*.

The index ξp, proposed to quantify the relative impact of factors other than PBD on the deviation between *CLTc* and *CLTt*, was calculated to be 61% using Eq. 4.

This indicates that while the PBD had a significant effect (39%), other process-related influences such as spatter formation and denudation also contributed substantially (61%) to the discrepancy between the computed and target consolidated layer thicknesses.

While isolating individual effects is complex, assessing the relative impact of PBD and other process factors offers valuable insights, especially when comparing parameter settings.

Finally, the distribution of local actual VED values is shown in Fig. 2-b, with a peak value of 12.8 J/mm³, an order of magnitude lower than the nominal VED of 111 J/mm³. This significant deviation reveals a reduced energy transmission efficiency for the investigated process setting.

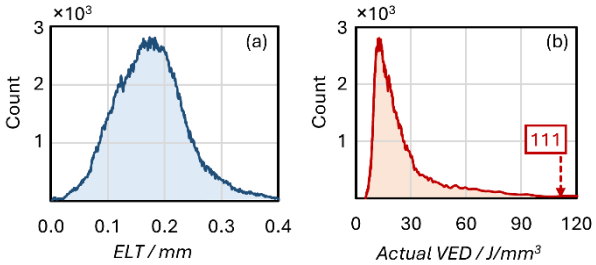

Figure 2. Distributions of values related to ELT (a), and actual VED (b). The nominal VED of 111 J/mm³ is indicated by a dashed arrow.

4. Conclusions

This work presented an experimental methodology to characterize local ELT, PBD, and actual VED in metal PBF-LB. For the investigated parameters (nominal VED: 111 J/mm³) and material (H13 tool steel), measurements revealed an order-of-magnitude deviation between the actual peak VED (12.8 J/mm3) and the nominal value, indicating a significantly reduced energy transmission efficiency. The mean ELT of 0.170 mm was 8.8 times the nominal layer thickness, with a standard deviation of 0.084 mm across the powder bed, quantifying the local variability linked to process stability. The ability to accurately and simultaneously measure ELT, PBD, and VED locally, and assess the relative impact of different process factors, can provide valuable insights into PBF-LB dynamics.

Future work will extend this approach to different materials and parameters, and integrate in-situ monitoring and simulation to develop a comprehensive framework for process control and quality assurance in metal additive manufacturing.

References

[1] Kruth, J.P., et al. (2007). Consolidation phenomena in laser and powder-bed based layered manufacturing. CIRP Annals, 56(2), 730–759.

[2] Zaeh, M.F., Ott, M. (2011). Investigations on heat regulation of additive manufacturing processes for metal structures. CIRP Annals.

[3] Wischeropp, T.M., et al. (2019). Measurement of actual powder layer height and packing density in a single layer in selective laser melting. Additive Manufacturing, 28.

[4] Amiri, M., Payton, E.J. (2021). An analytical model for prediction of denudation zone width in laser powder bed fusion additive manufacturing. Additive Manufacturing, 48, 102461.

[5] Eschner, E., Staudt, T., Schmidt, M. (2020). Correlation of spatter behavior and process zone formation in powder bed fusion of metals. CIRP Annals, 69(1), 209–212.

[6] Jansen, D., et al. (2021). Development of actual powder layer height depending on nominal layer thicknesses and selection of laser parameters. Journal of Materials Processing Technology, 298, 117305.

[7] Ali, U., et al. E. (2018). On the measurement of relative powder-bed compaction density in powder-bed additive manufacturing processes. Materials & Design, 155, 495–501.

[8] Zanini, F., Bonato, N., Carmignato, S. (2024). New multi-function building plate for improving metal laser powder bed fusion by enhancing the alignment accuracy of in-process monitoring data, computed tomography measurements, and building volume geometry. The International Journal of Advanced Manufacturing Technology, 132(5), 2369-2380.

[9] Zanini, F., Bonato, N., Carmignato, S. (2024). New experimental approach for local measurements of effective layer thickness, powder bed density and volumetric energy density to enhance metal laser powder bed fusion. Additive manufacturing, 93, 104432.